UCRL-51933

THE LLL TRANSIENT-ELECTROMAGNETICS-MEASUREMENT FACILITY

F. J. Deadrick, E. K. Miller and H. G. Hudson

October 29, 1975

Prepared for U.S. Energy Research & Development Administration under contract No. W-7405-Eng-48

LAWRENCE LIVERMORE LABORATORY
University of California/Livermore

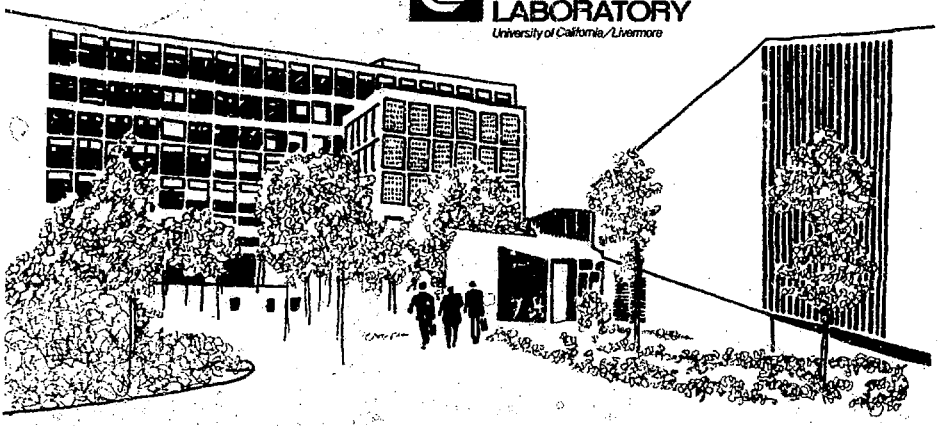

Printed in the United States of America
Available from
National Technical Information Service
U. S. Department of Commerce
5285 Port Royal Road
Springfield, Virginia 22151
Price: Printed Copy $___*; Microfiche $2.25

*Pages	NTIS Selling Price
1-50	$4.00
51-150	$5.45
151-325	$7.60
326-500	$10.60
501-1000	$13.60

Distribution Category
UC-38

LAWRENCE LIVERMORE LABORATORY
University of California/Livermore, California/94550

UCRL-51933

THE LLL TRANSIENT-ELECTROMAGNETICS-MEASUREMENT FACILITY

F. J. Deadrick, E. K. Miller and H. G. Hudson

MS. date: October 29, 1975

Contents

Abstract 1
Introduction 1
Principles of Operation 2
    Basic Measurement Procedure 2
    Capabilities 3
Transient-Measurement-Facility Hardware 4
    Ground Plane 5
    Source Antenna 5
    Pulse Generators 8
    Receiving Port 10
    Signal Sampling System 11
    Digital Computer Control System 12
Data Reduction and Processing 15
    Online Data Processing 16
    Offline Data Processing 16
    Time-Domain Reflectometry 19
    Equivalent-Circuit Characterization 21
    Model Scaling 21
Experimental Results and Validation 22
    Representative Measured and Calculated Results 23
Future Developments 27
    Sensing Probes 27
    Pulse Generators 28
    Instrumentation 28
    Computer Software 29
Acknowledgments 29
References 30

THE LLL TRANSIENT-ELECTROMAGNETICS-MEASUREMENT FACILITY

Abstract

This report describes the operation and hardware of the Lawrence Livermore Laboratory's transient-electromagnetics (EM)-measurement facility. The transient-EM range is useful for determining the time-domain transient responses of structures to incident EM pulses. To illustrate the accuracy and utility of the EM-measurement facility, actual experimental measurements are compared to numerically computed values.

Introduction

Short-pulse, wide-bandwidth, transient electromagnetics has been of both analytical and experimental interest for some time,[1-4] especially in connection with nuclear electromagnetic pulse (EMP) applications. It is only in the past few years, however, that capabilities have become available for achieving direct analytical time-domain solutions of EM problems. These time-domain solutions are generally based on integral equation formulations, are more complex than their frequency-domain counterparts, require fairly large digital computers, and are limited as yet to not-too-complex geometries of not-too-large a size compared to the highest frequency wavelength of the exciting field. Such time-domain solutions have proven especially useful in providing physical insight concerning the short-pulse behavior of simple structures; however, their applicability is not as broad as might be desired. For example, these solutions are not always useful in assessing an EMP interaction and coupling problem.

Therefore, there has been considerable emphasis in EMP work on developing simulators that can be used to measure the interaction of a complex structure (e.g., missile, building, airplane) exposed to a nominal EMP waveform. Simulator systems, with varying degrees of realism, can provide information on EMP-induced currents and voltages that can be expected at critical

points within a complex system. The simulator approach, however, is not generally as useful or flexible for making measurements requiring more basic applications, such as validating computed results or developing a data base for a set of representative interaction and coupling problems. This type of application is more appropriately satisfied by an experimental EM-measurement facility. Such a facility is also quite versatile as to the type of measurement that can be made. This report describes the development and operation of such an installation -- the LLL EM-measurement facility. Examples are given of the various kinds of measurements that can be performed at this facility along with numerically computed comparisons to evaluate the accuracy of the EM measurements.

Principles of Operation

Recent advances is subnanosecond pulse-generation and signal-sampling technology have created new EM-measurement techniques. Scale-model EM measurements, traditionally performed on a continuous wave (CW) basis in the frequency domain, now can be obtained through transient-response measurements in the time domain. Transient measurements offer several advantages over CW measurement techniques. For example, an expensive anechoic chamber is not needed to absorb unwanted reflections from the surrounding environment in indoor measurements. Also, the need for separate wideband magnitude and phase measurements is eliminated because this frequency-domain information can be obtained directly from a single transient-response measurement.

BASIC MEASUREMENT PROCEDURE

The design and operation of a transient measurement range are relatively simple. Our design, following that of Nicolson et al.,[5] consists of a large (8.5 × 8.5-m) ground plane against which a long (>4.3-m) wire (the transmit antenna) is driven by a short-duration (300 psec), high-amplitude (≈1.0 kV) impulse generator. The transmit antenna produces a hemispherical EM pulse that propagates outwardly from the feed region and illuminates the receiving antenna or scattering structure under test. The illuminating EM pulse excites the test structure, producing measurable signals characteristic of that structure. These signals are sensed by a pickup probe and fed through the

ground plane to a wideband (~10 GHz) sampling oscilloscope to produce a time-history record of the structure's pulse-excited transient response. The duration of the sampling window extends from the initial arrival time of the incident pulse to the time that unwanted reflections from the edge of the ground plane and the surrounding walls and ceiling appear at the target (typically 25 ns for our system). It should be noted that time-window sampling eliminates the need for an anechoic chamber; all measurements are completed before unwanted reflections appear in the data. Once the transient time-domain response data have been obtained, frequency-domain information can be calculated directly using the Fast-Fourier Transform (FFT) or, alternatively, derived from a complex exponential curve fit to the data. The latter technique, only recently been applied to EM problems, is based on Prony's algorithm. This technique will be discussed later in the "Data Reduction and Post-Processing" section.

CAPABILITIES

Transient-EM-modeling techniques of the type described in this report are applicable to a variety of problems involving electromagnetic radiation, propagation, and scattering, The techniques are particularly well suited to bodies exhibiting mirror symmetry and where the measurement is made at the plane of symmetry (i.e., a free-space dipole of length ℓ is modeled as a monopole of length $\ell/2$ attached to the ground plane). Typical transient EM measurements include:

- Bistatic and monostatic scattering
- Wideband terminal impedances via time-domain reflectometry (TDR)
- Wideband antenna-radiation patterns
- Aperture coupling
- "Infinite-structure" surge impedances
- Discrete and distributed loading
- Nonlinear loads (i.e., diodes)
- Pulse-excited transient response
- Short-circuit current response
- Open-circuit voltage response
- "Free-space" response
- Structure response over perfect ground.

Transient-Measurement-Facility Hardware

The basic components of the LLL transient-EM-measurement facility are shown in Fig. 1. An aluminum-covered platform serves as the ground plane. As shown, a transient EM pulse is radiated by the long conical antenna, which is driven by a high-voltage impulse generator. The transmitted field of this antenna illuminates the test target. The resulting induced response is then picked up by a probe and fed to a very wide bandwidth

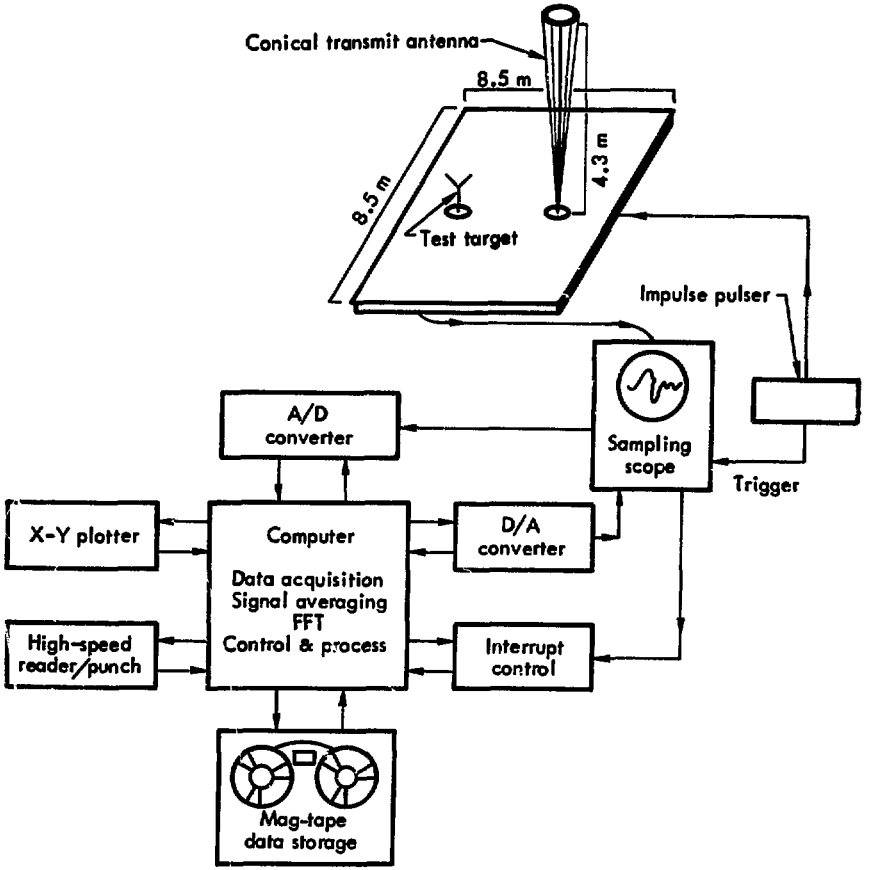

Fig. 1. Schematic of LLL transient EM-measurement facility.

oscilloscope, which samples many repetitive pulses to record the temporal response of the target. A digital computer controls the experiment, obtains the transient data from the sampling oscilloscope, processes the data, stores it in core for online processing, and records the data on magnetic tape for later offline processing. A more detailed description of the system is presented in the following sections.

GROUND PLANE

The ground plane used at the LLL transient-EM range is shown in Fig. 2 Sheets of 1/8-in.-thick aluminum are attached to the elevated platform to form an 8.5 × 8.5-m "perfect" image ground plane. The use of a ground plane has several advantages, chief of which is the fact that instrument-caused field perturbations can be effectively isolated from the experiment by placing all instrumentation below the image plane. Symmetric structures (e.g., dipoles) are then modeled as monopoles over the ground plane, with the ground image forming the other half of the structure.

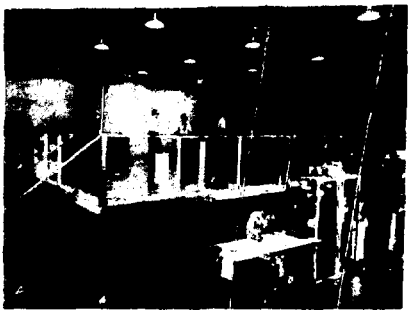

Fig. 2. Ground plane and data-acquisition equipment.

The size of the ground plane plays an important role in establishing the total clear-time (sample window) available for the measurement. Clear-time is primarily determined by the time it takes an EM pulse to reflect off the edge of ground plane or the surrounding walls or ceiling and return to the target area. For our facility (Fig. 2), clear-time is typically about 25 nsec.

As shown in Fig. 3, the elevated ground plane allows instrumentation to be placed directly beneath the experimental area. There is also sufficient clearance for personnel to work below the test area. A plan layout of the facility is shown in Fig. 4.

SOURCE ANTENNA

A transmit antenna is used to generate an incident transient field at the target. This source antenna consists of a conical structure formed by nine azimuthally symmetric wires with a 10-deg cone angle. The upper cone with its ground image forms a

Fig. 3. Instrumentation below experimental area.

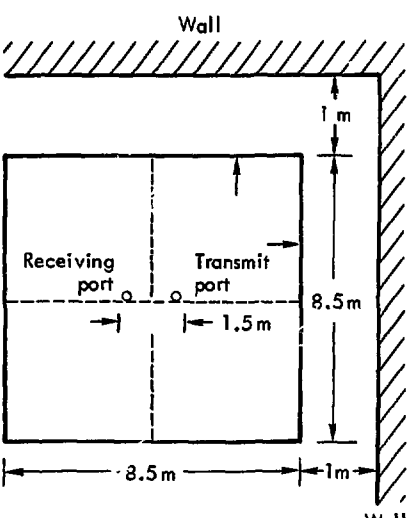

Fig. 4. Plan layout of LLL transient EM-measurement facility.

biconic structure. A bicone antenna is particularly well suited to transient-type excitation for several reasons. First, for cones of infinite extent (the case before any reflections from the far end of the cone return to the source), the antenna is frequency independent (i.e., it looks like a transmission line). A spherical wave front, like that shown in Fig. 5(a), is generated in the source-feed region. The field produced by the bicone is a pure transverse EM wave (electric and magnetic field lines lie in a direction transverse to the direction of propagation) traveling outward with a free-space velocity c.

The input impedance of a bicone is given by:[6]

$$Z_{BICONE} = \frac{\eta_0}{\pi} \ln\left(\cot\frac{\psi}{2}\right), \qquad (1)$$

where η_0 = impedance of free space = 377 Ω and ψ = bicone half-angle. For a 5-deg half-angle bicone, the bicone impedance is 375.8 Ω, very near that of free space.

The electric field produced by a bicone antenna (see Fig. 5a) can be computed as follows.[6] Consider only an outward-propagating pulse from the

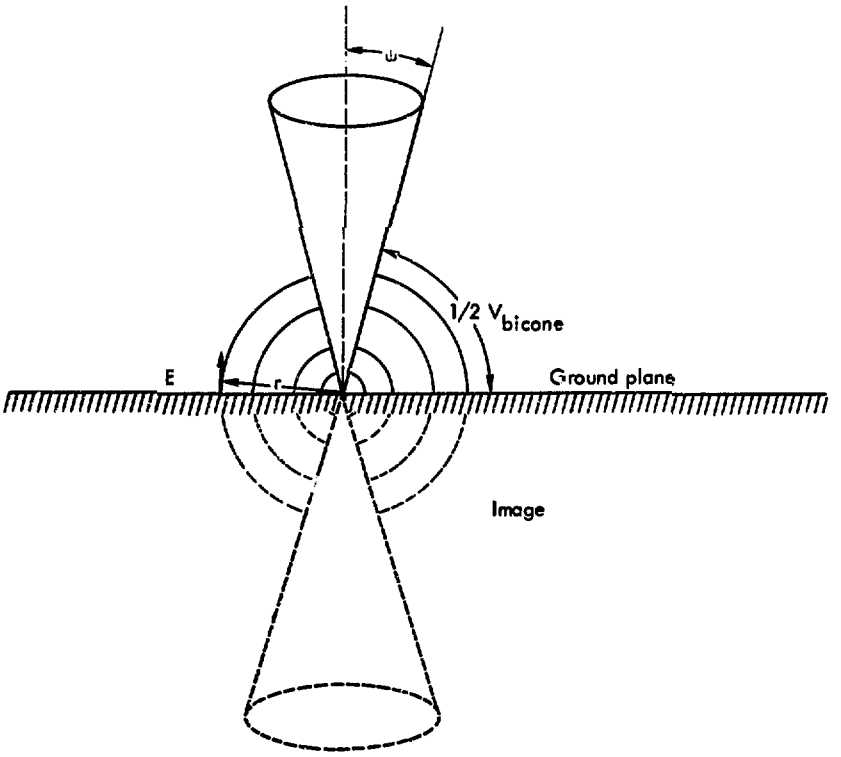

(a) Bicone antenna over ground plane with image

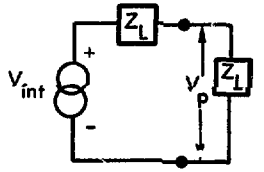

(b) Pulser-voltage measuring circuit

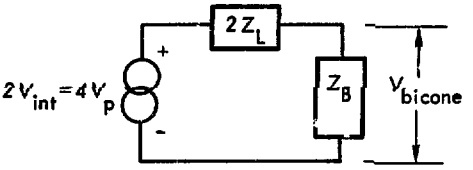

(c) Equivalent bicone circuit

Fig. 5. Bicone transmit antenna.

source region. One has, in spherical coordinates,

$$E_r = 0$$

$$rE_\theta = \frac{\eta}{\sin\theta}\left[Ae^{j(\omega t - kr)}\right]$$

$$rH_\phi = \frac{1}{\sin\theta}\left[Ae^{j(\omega t - kr)}\right].$$

Since E_θ corresponds to the voltage difference between the two cones,

$$V_{bicone} = -\int_{\psi}^{\pi-\psi} E_\theta r d\theta$$

$$= 2\eta \ell n \cot\frac{\psi}{2}\left[Ae^{-j(\omega t - kr)}\right].$$

Hence, the electric field at $\theta = \pi/2$ (on the ground plane) can be written

$$E_\theta(r) = \frac{V_{bicone}}{2r\ \ell n\ \cot(\psi/2)}\ .$$

Pulser voltage V_p is defined by the circuit in Fig. 5(b), where Z_L is the pulser terminal impedance. Note that V_p is also measured with an instrument of terminal impedance Z_L. The E_θ field can then be related to the pulser voltage as shown in Fig. 5(c).

$$E_\theta(r) = \frac{2V_p}{\ell n\ \cot(\psi/2)}\left[\frac{Z_{bicone}}{Z_{bicone}+2Z_L}\right]\frac{1}{r}\ . \quad (2)$$

PULSE GENERATORS

Transient-response measurements naturally are proportional to the output of the pulse generator driving the system. Ideally, one wants a pulse generator with a wideband (~2 decades), frequency-independent, high-amplitude output. Such pulse generators are difficult to obtain; however, we have found two different pulsers to be useful. The fastest available is the IKOR IMP impulse generator,* which has a nominal 1-kV output into a 50-Ω load, with a gaussian-shaped waveform 300 psec wide at its mid-height. A typical pulse waveform from this generator is shown in Fig. 6. The spectral content of this pulser is shown in Fig. 7.

As an alternative to the IKOR generator, we use a Tektronix 109 mercury-reed-switched pulser. This pulser has a 40-V output with pulse widths of less than 1 nsec (using the unit's internal charge line). The

*Reference to a company or product name here or elsewhere in this report does not imply approval or recommendation of the product by the University of California or the U.S. Energy Research & Development Administration to the exclusion of others that may be suitable.

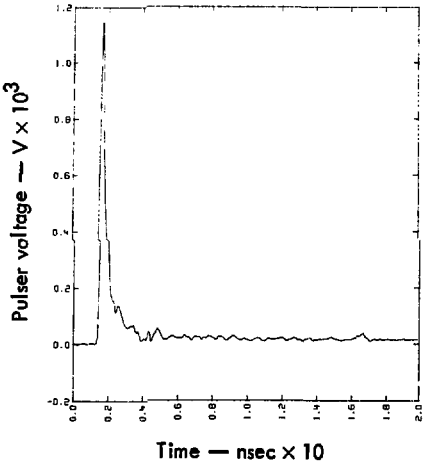

Fig. 6. Typical pulse waveform from IKOR IMP impulse generator.

pulse output and spectrum of this pulser are shown in Figs. 8 and 9, respectively.

From the standpoint of improved signal-to-noise ratios, high pulse amplitudes are desirable, particularly if one is interested in measuring attenuation through various media. Narrow, fast risetime pulses are desirable both to produce wide-bandwidth excitation and to produce the narrow spatial pulse required to resolve fine detail in the experimental target.

In a repetitive time-sampled system as used here, it is also extremely important that each pulse

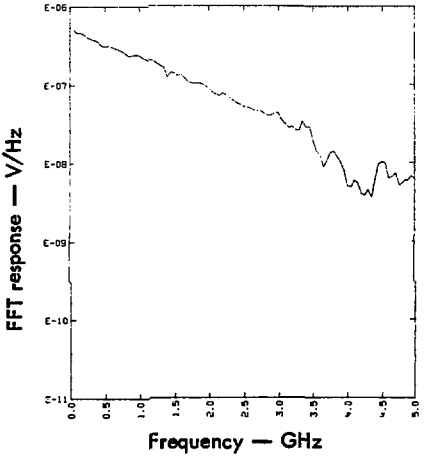

Fig. 7. Spectral content of pulse waveform shown in Fig. 6.

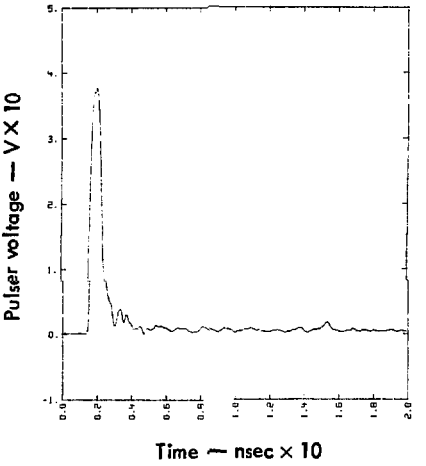

Fig. 8. Pulse waveform from Tektronix 109 impulse generator.

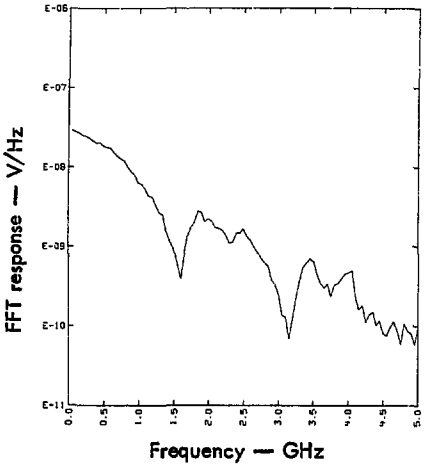

Fig. 9. Spectral content of Tektronix pulse output shown in Fig. 8.

be of uniform amplitude and form, with little jitter in the time-base trigger circuitry.

RECEIVING PORT

The receiving port (location at which the transient response is sampled) is typically a point on the image ground plane (see Fig. 10). The aircraft model is connected to a sampling oscilloscope by a 50-Ω coaxial cable (Fig. 11). The signal recorded by the sampling oscilloscope is the current injected into the cable's 50-Ω load impedance by the target's excitation.

An alternative measurement technique is to use a current transformer, such as the Tektronix CT-1, which measures actual target current. This technique permits direct measurement of the short-circuit current induced on a structure as long as the probe introduces no appreciable loading on the target.

Resistive loading may also be added to the structure by using lumped resistors. We have found

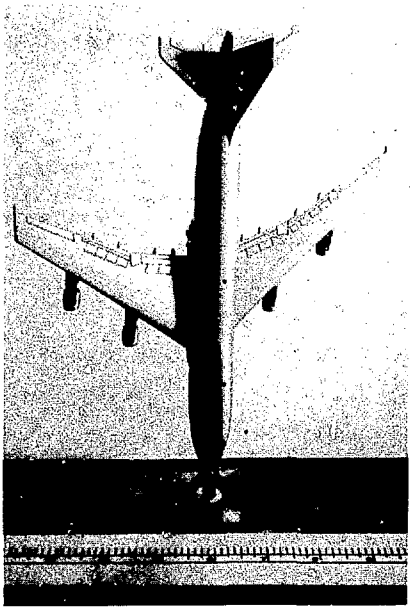

Fig. 10. Scale model connected to receiving port on ground plane to measure nose current.

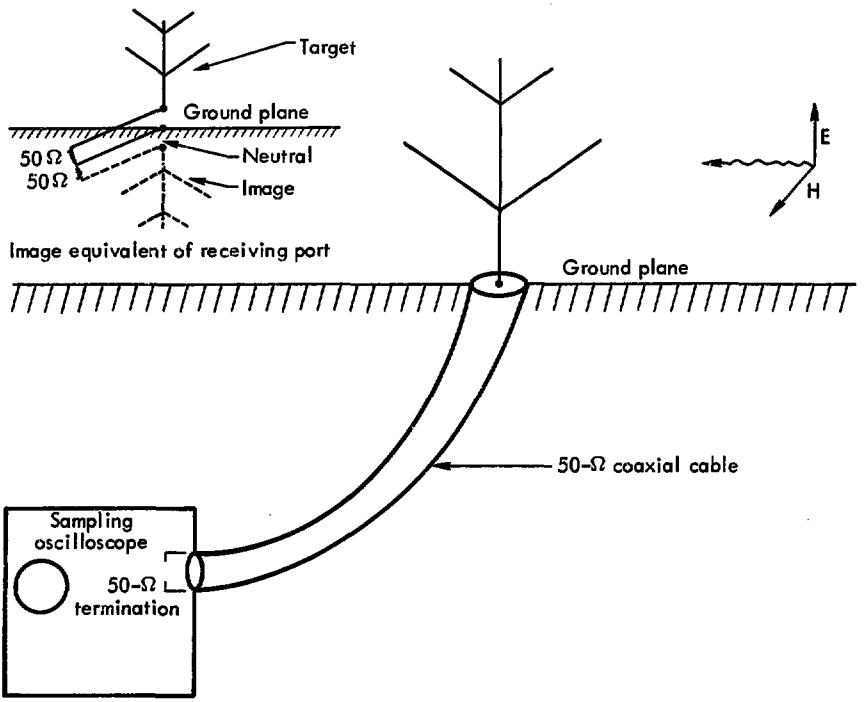

Fig. 1. Diagram shows physical configuration of receiving port on ground plane. Also shown is the connection between target and sampling oscilloscope.

resistive loading particularly useful in damping out late-time transient response, thereby enabling a shorter sample to be taken in the limited sample window. Resistive loading also allows larger structures to be measured and the loading effects can be easily removed from the measured data later in off-line processing.

SIGNAL SAMPLING SYSTEM

A very significant advancement in high-frequency measurement techniques is the sampling oscilloscope. This measurement technique is very similar, in principle, to the use of stroboscopic light to study fast mechanical motion. Progressive samples of

adjacent portions of successive waveforms are recorded and then "stretched" in time, amplified by relatively low-bandwidth amplifiers, and finally displayed (one sample at a time) on a cathode-ray-tube (CRT) screen. The CRT then produces a replica of the sampled waveforms.

The principal difference between conventional displays and those made by sampling techniques is that sampling displays are composed of separate segments or dots. The sampling technique is limited therefore to depicting repetitive signals because only one sample is taken and displayed each time the signal recurs. Nonetheless, this sampling method provides a means for examining fast-changing, low-amplitude signals that cannot be examined in any other way.

For each dot on the CRT, an analog signal is produced proportional to the sampled signal's amplitude. A pulse output is also generated after the sample is available and ready to be read by the computer. These two pieces of information are used as inputs to the on-line digital computer, which in turn converts the oscilloscope's analog output to a digital format. (A more detailed description of this system is given in the next section).

The sampling oscilloscope also allows the position on the time base where samples are taken to be controlled. And, if desired, this position can be fixed to make repetitive samples in the same relative time frame. This technique is used to average the signal before going on to the next step time. An analog voltage input to the oscilloscope controls a sample's time position; we are able to obtain, for example, 512 equally spaced time samples across the CRT time sweep.

A block diagram of the sampling oscilloscope system, with associated module risetimes is shown in Fig. 12. A Tektronix 7408 scope mainframe, with a 7T11 time base, a 7S11 sampling unit, and an S4 sampling head make up the scope system. In addition, a Tektronix 7M11 time delay unit is used for some measurements. The trigger source for the system is obtained from the pulser output through a Tektronix CT-3 signal pickoff unit.

DIGITAL COMPUTER CONTROL SYSTEM

A digital computer plays a dominant role in operating the time-domain range; in fact, it controls the whole experiment. The experiment-control computer program does several things; it:

- Asks the experimenter for run descriptions and scope-calibration factors

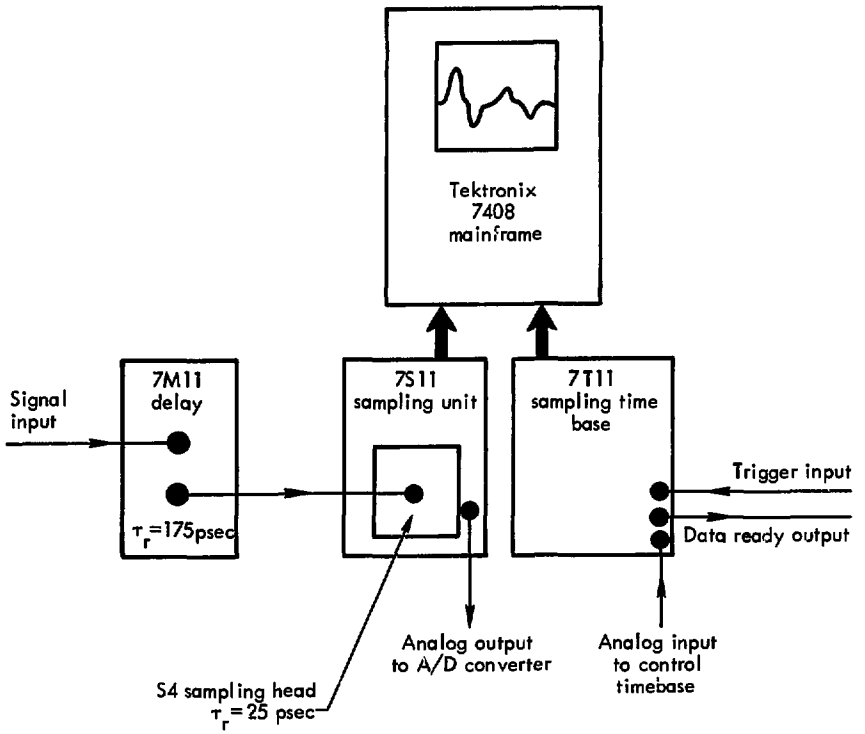

Fig. 12. Block diagram of sampling oscilloscope system.

- Plots results (including scales and titles) on an online Calcomp plotter
- Records accumulated experimental data on magnetic tape for later offline post processing
- Controls the sampling oscilloscope as to where in the time history samples should be taken and how many samples to take at each point.

The data-gathering portion of the control program is perhaps the most important in terms of operating the time-domain range. Each time the pulser is triggered, the sampling oscilloscope obtains a discrete time-step sample of the transient waveform. For each sample, the oscilloscope

provides an analog output proportional to the sampled value. The oscilloscope also generates a pulse output at the time when the analog output is ready for external measurement. These two oscilloscope signals are input to the computer.

The pulse output is used to interrupt the computer's background program, signaling that an analog output of the sampled signal is available. This analog signal is first converted to a digital format (12 bits resolution in 20 μsec). The data is then checked for "glitches" by comparing its input value with time samples at the previous time step. If the difference between successive samples is greater than allowed, the sample is discarded.

At each time step, several time samples (generally 10 to 20) are averaged* to give a mean data value and to improve the overall signal-to-noise ratio.[7] The program only stores the averaged data points for each time step, and, for convenience in using the FFT, the trace is divided into 512 equally-spaced time steps.

*A more sophisticated scheme would be to compute the variance of the samples contributing to the data point and discontinue the sampling when it fell below a preset limit. This technique will be incorporated in future designs.

The computer also sends a signal back to the oscilloscope to control the time-step position at which the next time sample is to be taken.

When all 512 time steps have been obtained, the data is plotted by

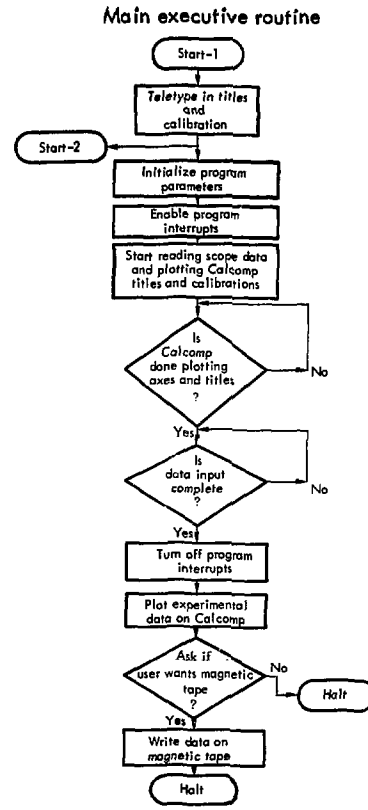

Fig. 13. Flow chart of data-acquisition and experiment-control computer program.

Data-acquisition interrupt/service routine

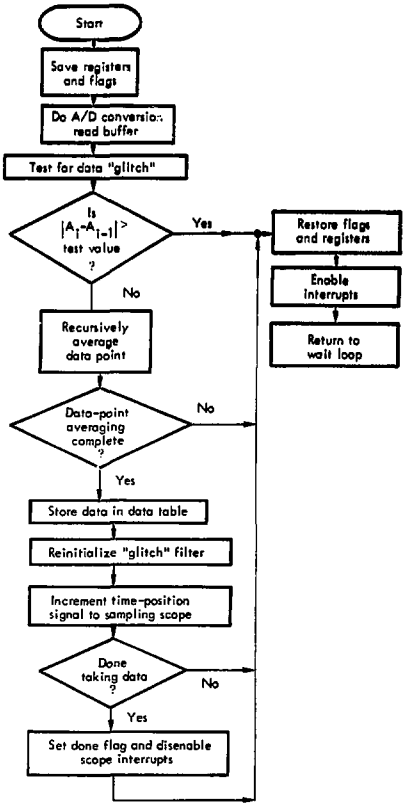

Fig. 13. (Continued.)

Calcomp plotter and recorded on a magnetic tape for later offline post processing on a larger scientific computer. Typically, 512 time-step samples are collected in less than 45 sec. A flow chart of the data-acquisition and experiment-control computer program is shown in Fig. 13.

Calcomp interrupt/service routine

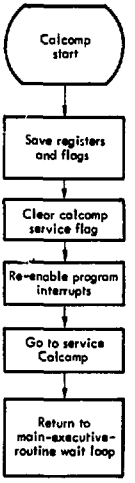

Fig. 13. (Continued.)

Data Reduction and Processing

In the previous section, we described the hardware used to collect transient data at the LLL EM-measurement facility. Here we discuss how the data are processed, both on- and offline. A few simple scale-model experiments are used to demonstrate the system operations.

ONLINE DATA PROCESSING

The computer used to control the time-domain-range hardware can also perform a limited amount of online data processing. For example, using the FFT, the computer can convert time-domain data directly to its frequency-domain equivalent. This online transform capability is useful in that it provides a quick frequency-domain look at time-domain data.

The computer is of the PDP-8I class, with a hardware multiply and divide unit and a 12-K 12-bit core memory. As mentioned in the previous section, the online data-acquisition program obtains 512 equally spaced discrete data points to represent the transient waveform. Each data point is the average of a number of signal time samples, and an online averaging technique is used to improve the signal-to-noise ratio. All 512 data points are stored in the computer core memory and, after all data have been acquired, the points are plotted by Calcomp.

For most applications, however, it is preferable to have a permanent record of the data and to process the data further on a larger, more flexible computer. Because of speed and the control of I/O operations, assembly language is used in the minicomputer data-acquisition system, although it is not as easy to change as FORTRAN or some other higher-level language.). All experimental data are recorded on a digital magnetic tape. A file is devoted to each run. In this file are three descriptive records; one contains voltage calibration information, another time-calibration factors, and the last a description of the data contained in the file. The remainder of the data file contains the data records. These magnetic-tape records can be further processed offline by one of our larger scientific computers (CDC 7600s).

OFFLINE DATA PROCESSING

The ability to process the experimental data offline is particularly advantageous when additional manipulation of raw data is required or when it is desirable to plot the experimental data in a different format at a later date. Typical examples of offline processing are described in the following paragraphs.

It is often desirable to convert time-domain transient data to its frequency-domain equivalent. A common way to do this is to use the FFT. If the time-domain data record is T_{max} seconds long it is sampled at intervals Δt seconds apart, the corresponding frequency-domain data record obtained using FFT will extend from zero to a maximum frequency $f_{max} = 1/2\Delta t$ Hz with samples spaced $\Delta f =$

$1/T_{max}$ apart. To get more closely spaced samples in the frequency domain, T_{max} must be increased. This can be done by measuring the transient response over the maximum time interval allowed by the measurement free time. For a time response that has decayed to zero, Δf can be further decreased by adding zero-value data samples to it (zero filling).

The highest useful frequency in the frequency-domain data cannot exceed f_{max}. Generally, however, it will be less than f_{max} because the maximum useful frequency is determined by the highest frequency available in the exciting pulse and the response of the test object. While using a Δt smaller than the minimum required has no significant impact on data-acquisition time, it provides more flexibility in subsequent data processing and it ensures that useful information is not missed. A typical example of a transient-response waveform and its frequency-domain equivalent is shown in Figs. 14 and 15.

There are other ways of obtaining frequency-domain information from transient data. A particularly intriguing approach is to use an exponential curve-fitting process based on Prony's algorithm. This technique is based on the premise that time-dependent data can be fit by a sum of complex exponentials, i.e.,

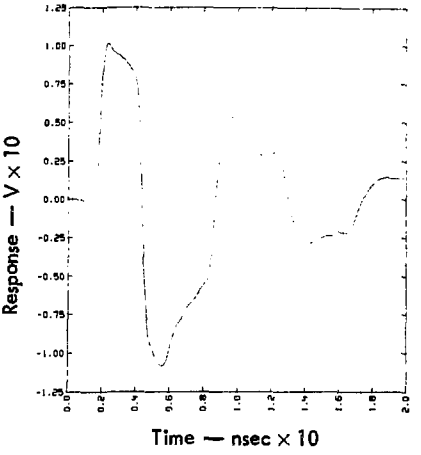

Fig. 14. Transient-response waveform of 60-cm monopole on ground plane.

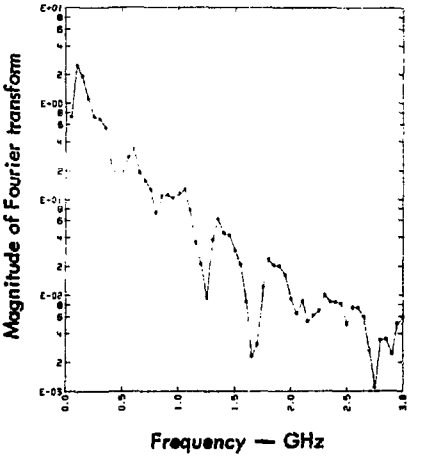

Fig. 15. Frequency-domain equivalent of the 60-cm-monopole transient response shown in Fig. 14.

$$f(n\Delta T) = \sum_{i=1}^{K} A_i e^{\alpha_i n\Delta t}, \qquad (3)$$

where α_i, i=1, 2....K, ($K \leq N/2$) are the complex poles of a polynomial equation used in the Prony solution and A_i is the complex amplitude or residual found in fitting the data with a least-squares-curve fit.

Equation 3 has several unique properties that make it useful. First, it allows extrapolation of the time-sampled function to times later than those measured. Thus, it is possible to extrapolate the time response to times greater than the normal 25-nsec experiment sampling window or the free time of the ground plane. It is even possible to extrapolate backwards in time. Examples of both forward and backward extrapolation are shown in Fig. 16 for results derived from a calculated waveform. Note, however, that the extrapolation works over the time interval where the exciting pulse is no longer present.

Another feature of this exponential form (Eq. 3) is the simple frequency-domain transform that results from using the complex exponents and coefficients given in Eq. 4:

$$F(s) = \sum_{i=1}^{K} \frac{A_i}{(s-\alpha_i)}, \qquad (4)$$

where $s = j\omega$.

Figure 17 shows the frequency-domain transform given by this method. The comparable FFT for the same transient response is shown in Fig. 18. One advantage of Eq. 4 over the conventional FFT method is that this transform permits continuous frequency variation rather than the discrete sampling imposed by FFT. A penalty is paid with the use of this method, however, in terms of computation time.

A comparison of complex pole sets, α_i, obtained for a straight wire from a computed waveform response is shown in Fig. 19. The locus of these poles is comparable to those found via the Singularity Expansion Method (SEM).[8]

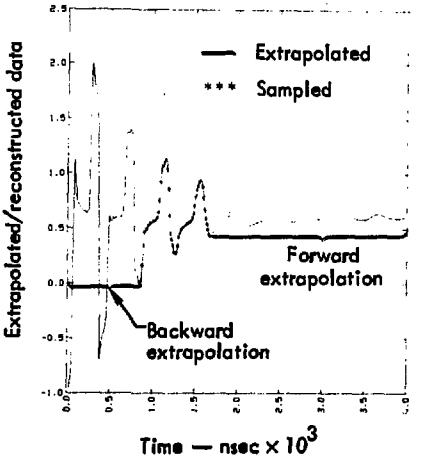

Fig. 16. Example of forward and backward extrapolation of a finite data sample.

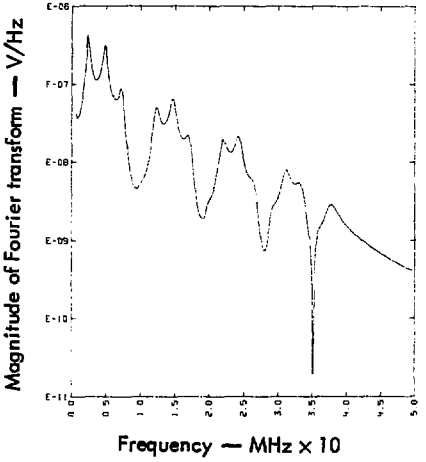

Fig. 17. Frequency-domain transform as determined by Prony method.

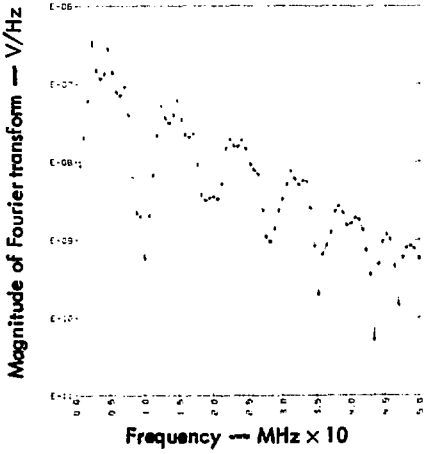

Fig. 18. Frequency-domain transform as determined by FFT method.

TIME-DOMAIN REFLECTOMETRY

Time-domain-reflectometry techniques, quite common in the analysis of transmission lines and networks, are also applicable to EM measurements. In particular, TDR techniques offer a simple way of determining the port impedance of an antenna from two transient measurements. First, the voltage pulse reflected from the input terminal of the structure being tested is measured after it is excited as an antenna, which provides its input impedance. The measurement is then repeated only this time the test structure is replaced by a standard load of known value (e.g., a short circuit). Figure 20 shows the experimental setup for TDR measurements.

The reflected voltage waveforms for both the short circuit and the unknown load are then transformed to the frequency domain, and a frequency-dependent reflection coefficient is computed as follows:

$$\rho(f) = -\frac{V_{LOAD}(f)}{V_{SHORT}(f)} . \qquad (5)$$

With a knowledge of $\rho(f)$, port impedance as a function of frequency is then given by

$$Z_{in}(f) = \frac{1 - \rho(f)}{1 + \rho(f)} * Z_o , \qquad (6)$$

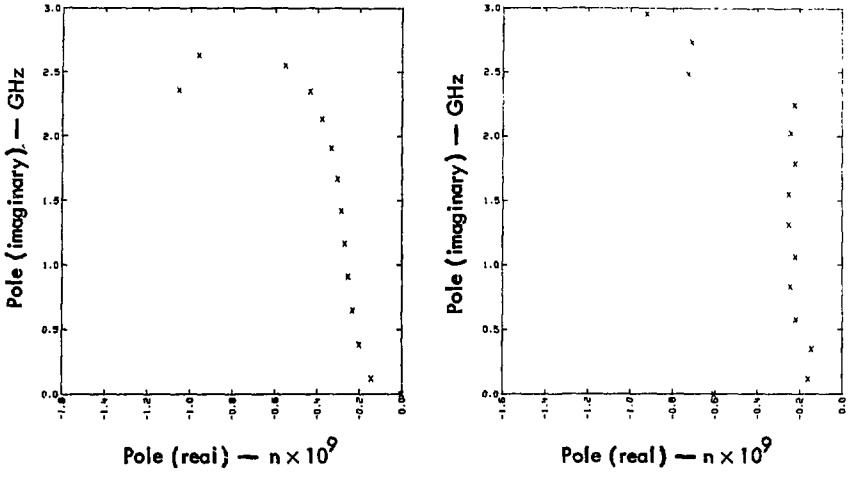

Fig. 19. Comparison of measured versus calculated pole sets for a straight-wire target.

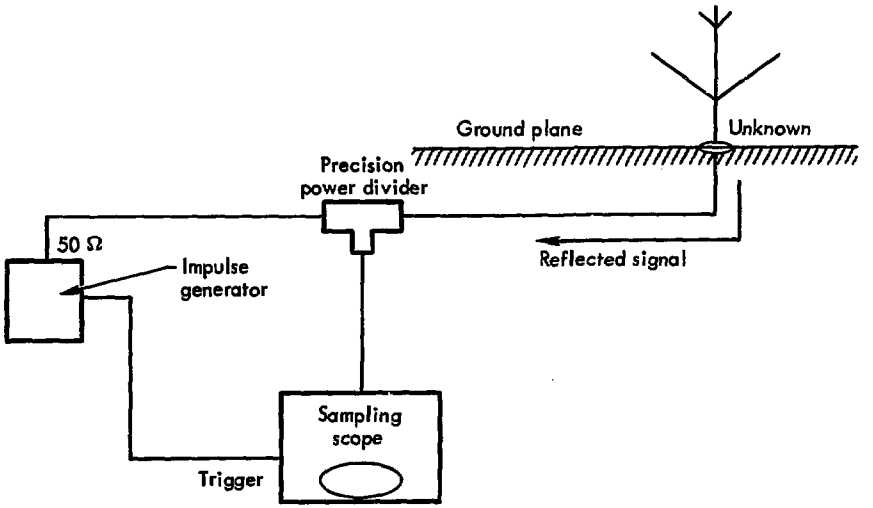

Fig. 20. Experimental setup for TDR measurements.

where Z_o is the characteristic line impedance used in the experiment. In our case, $Z_o = 50\Omega$. Results obtained using the TDR technique are presented in the section on Experimental Results and Validation.

EQUIVALENT-CIRCUIT CHARACTERIZATION

Energy collectors such as antennas are conveniently modeled in terms of an equivalent circuit, as shown in Fig. 21. In this figure, Z_a is the terminal impedance characteristic (found using TDR techniques), E_{INC} is the incident field in volts per meter, and h_{eff} is the effective height of the structure under test. We can determine all of the parameters needed for this model experimentally. To determine effective height, a scattering experiment is performed in which the conic transmit antenna is driven with a narrow pulse and the induced response of the antenna under test is measured. Referring to Fig. 21, Z_L is the characteristic impedance of the transmission line that connects the sampling oscilloscope to the antenna (50Ω in this experiment). It represents the load across which the voltage is measured. The remaining quantity, E_{INC}, can be determined by Eq. 2 for a given pulser voltage waveform. Thus, knowing $E_{INC}(t)$, $Z_a(f)$, and $V_L(t)$, we can find $h_{eff}(f)$ in the frequency domain as follows:

$$h_{eff}(f)\ E_{INC}(f) = Z_a(f)\ I_L(f) + V_L(f), \qquad (7)$$

where

$$I_L(f) = \frac{V_L(f)}{Z_L},$$

so that

$$h_{eff}(f) = \frac{(Z_a + Z_L)\ V_L(f)}{Z_L\ E_{INC}(f)}.$$

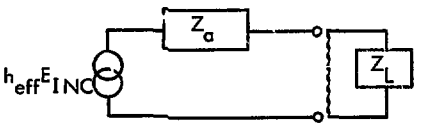

Fig. 21. Frequency-domain-equivalent circuit of an antenna.

MODEL SCALING

Laboratory scale models can be used to predict the characteristics of full-scale structures when they are both perfectly conducting. When scaling in size, a scale factor can be defined as $SF = \frac{Size_{STRUCTURE}}{Size_{MODEL}}$. The effective height will scale as

$$h_{eff_{STRUCTURE}}(f) = h_{eff_{MODEL}}(f) * SF \qquad (8)$$

and the frequency will scale as

$$f_{STRUCTURE} = f_{MODEL}/SF. \quad (9)$$

The term Z_a does not scale, only the frequency at which it is defined is scaled, i.e.,

$$Z_{a_{MODEL}}(f) = Z_{a_{STRUCTURE}}(f/SF).$$

Thus, the equivalent circuit in Fig. 21 can be scaled to any arbitrary size and the load Z_L can be varied to analyze a variety of situations from a single measurement.

Experimental Results and Validation

An experimental facility is often a useful tool for validating numerical modeling codes, comparisons are routinely made between numerical and experimental results. An experimental facility can also complement a numerical capability. For example, it is often easier to model a complex structure experimentally than to do so numerically. In fact, it may not be possible to numerically model some structures. To demonstrate these points, this section presents results obtained at our transient EM-modeling facility that have been used to validate and complement theoretical models. In these examples, numerical results are given for comparison wherever practical.

REPRESENTATIVE MEASURED AND CALCUALTED RESULTS

Much of LLL's interest in transient EM stems from our ability to compute transient EM responses using the computer code WT-MBA/LLL1B.[2] This code, based on a time-dependent integral-equation formulation of Maxwell's equations, allows us to numerically model structures that can also be experimentally tested in the laboratory. The simplest of these structures is the linear dipole (or monopole, when located over a perfect ground plane).

Figures 22a and 22b show the calculated and experimental transient feed point currents excited on a 20-cm and a 1-m monopole when illuminated by a gaussian-shaped pulse incident field. The comparison is quite good. It should be noted that the numerical results were obtained by modeling the complete experimental setup, including the transmitting-source antenna* and using the pulser voltage waveform to drive the transmit antenna as in the actual experiment.

*The transmitting antenna used in these experiments was a single straight wire.

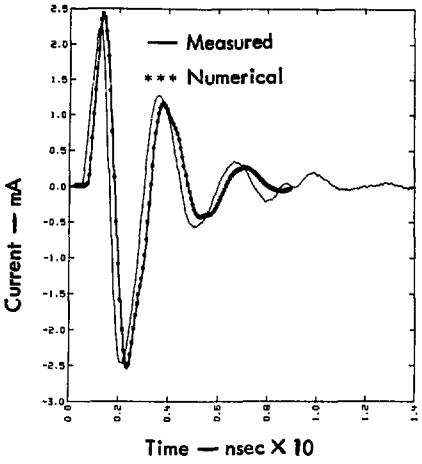

Fig. 22a. Experimental and numerical currents on a 20-cm monopole.

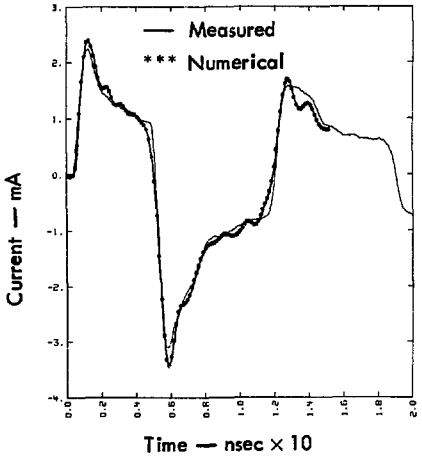

Fig. 22b. Experimental and numerical currents on a 1-m monopole.

Also in Figs. 22a and 22b, observe that the "noise" in both the measured and calculated waveforms (especially evident in the 1-m case) is due to similiar noise on the applied voltage pulse (see Fig. 8, the Tektronix 109 pulser output). For comparison, a calculated response from a smooth applied gaussian pulse is shown in Fig. 23.

Figure 24 shows computed and experimental results for a slightly more complex structure. The antenna modeled is a dipole with V-shaped end loads. Again, computed results were obtained using the WT-MBA/LLL1B code, as described above. The parameter plotted in these figures is the current that flows through a 100-Ω load in the center of the V-dipole or the 50-Ω coaxial cable line termination in the experimental setup of the half V-dipole when it is modeled over the ground plane. Again, there is good agreement between experiment and analysis. (In this case, an error was discovered in our experimental setup; the time base used for the sampling oscilloscope was out of calibration, causing the slight time shift evident between the two curves as shown in Fig. 24.)

The above examples lend confidence to both the experimental and, numerical treatment of the EM problem. With this confidence, we plan to

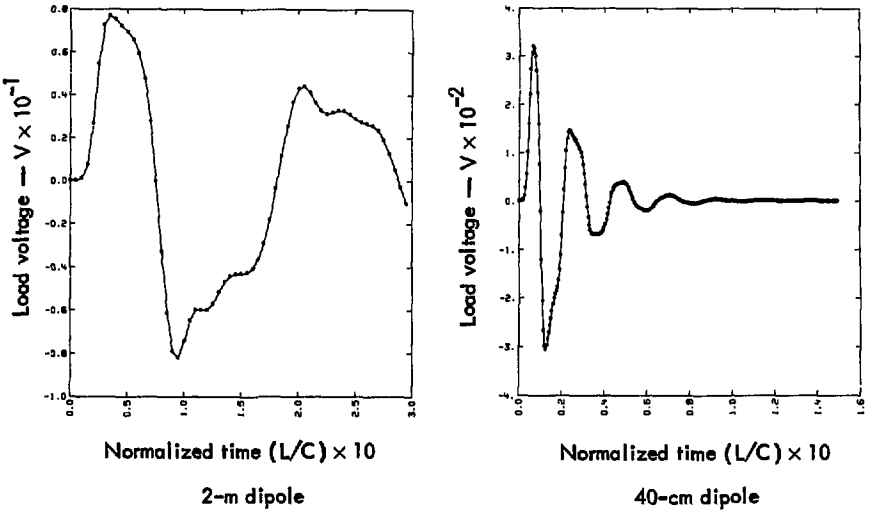

Fig. 23. Computed transient response of a 40-cm and a 2-m dipole excited by an incident broadside gaussian pulse (300 psec wide).

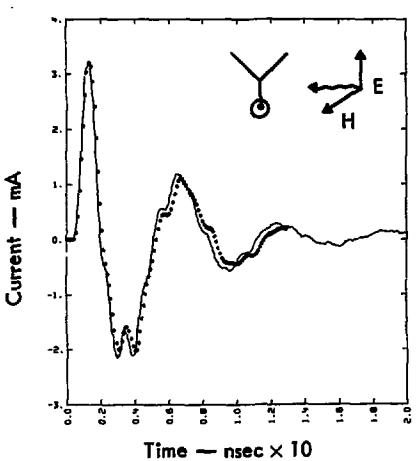

Fig. 24. Comparison between computed and experimental results for a dipole with V-shaped end loads.

extend our techniques to more difficult problems, such as the scattering behavior of an aircraft when illuminated by an incident nuclear EMP. Obviously, it would be extremely difficult to develop a complete numerical model of such a large structure as an aircraft; therefore one must look for ways of simplifying the numerical model. Scale-model measurement, it turns out, is a convenient way of studying numerical models to determine what constitutes a good model and to show what model relationships are involved. Figure 25 shows three models of a

747 jetliner. The model in the center is a 1/247-scale model of the actual aircraft. Those on either side are stick models, which can more easily be treated by our thin-wire time-domain modeling code. To see how well the thin-wire model approximates the scale model is simply a matter of making the experimental comparison shown in Fig. 26a and 26b for both the time and frequency domains. On a bulk basis, the three structures have similiar response characteristics in both the time and frequency domains. The "fatter" scale model has a higher peak current than either of the "computer" models due to its larger energy-collection area. In the wire models, peak current decreases as wire diameter is decreased. Figure 27 shows the experimental and calculated response for the 1/4-in. pipe model.

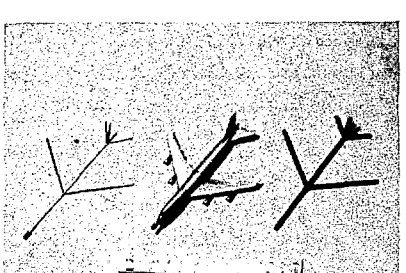

Fig. 25. Scale and "computer" models of Boeing 747 aircraft.

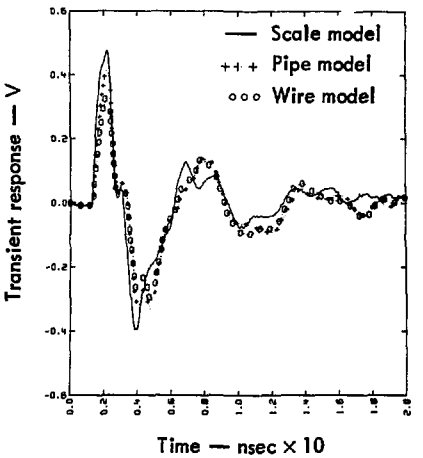

Fig. 26a. Transient responses for each of the aircraft models shown in Fig. 25.

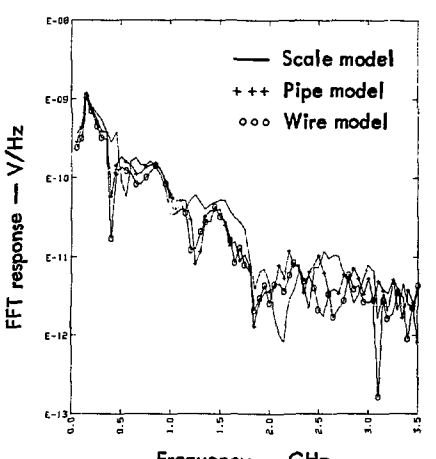

Fig. 26b. Frequency-domain responses for each of the models shown in Fig. 25.

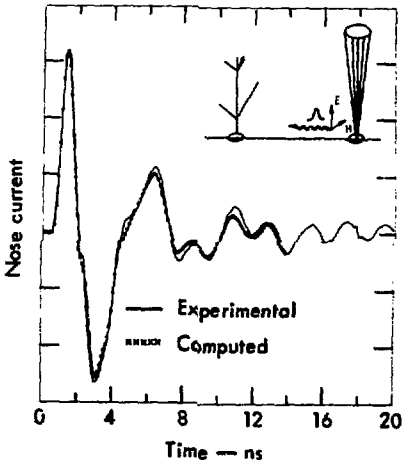

Fig. 27. Comparison between experimental and calculated nose current on the 1/4-in.-pipe model.

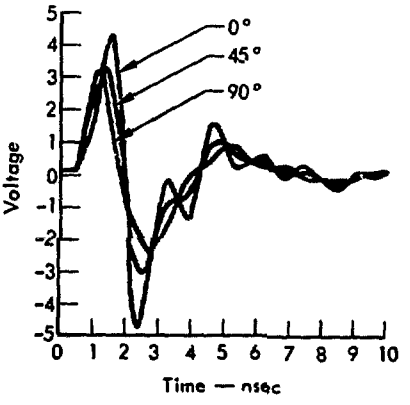

Fig. 28. Transient response of U-shaped antenna for various azimuth angles.

Transient EM measurements can also be used to study antenna radiation (or receiving) patterns. A single transient measurement can give the directional properties of a radiator over a wide range of frequencies. Figure 28 illustrates the transient response of a U-shaped antenna for several azimuth angles. This temporal data may also be transformed to the frequency domain to give the radiation properties of the structure at a particular frequency.

As mentioned in the previous section, time-domain reflectometry is a convenient way of determining the wideband port or input impedance of a device. Figures 29 and 30 show the input impedance of 60-cm monopole antenna over a perfect ground plane, along with numerically computed input-impedance results obtained using the WT-MBA/LLL1B code. As shown by Figs. 29 and 30, both the resistance and reactance of the antenna are reasonably well determined by this technique, and, for the structure studied, roughly 10 resonances can be defined.

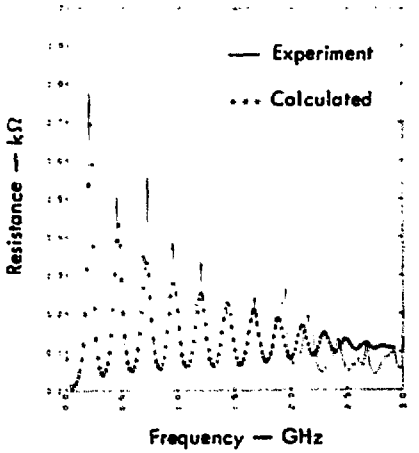

Fig. 29. Input resistance of 60-cm monopole, as determined by TDR technique.

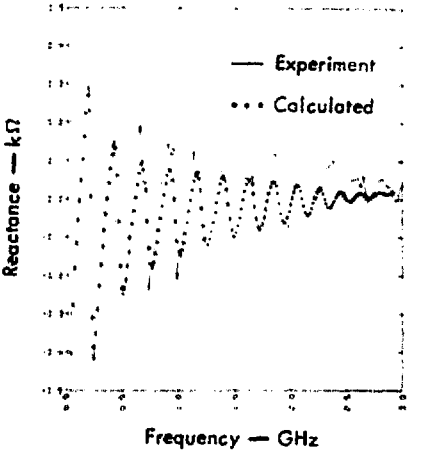

Fig. 30. Input reactance of 60-cm monopole, as determined by TDR technique.

Future Developments

The capabilities provided by the transient range at its present stage of development, though indeed useful, could be extended substantially with further hardware and software improvements. Some of improvements being considered are presented in the following sections.

SENSING PROBES

One of the most severe limitations of the present range is the fact that measurements generally must be made at the ground plane. This restriction precludes the possibility of determining, for example, current distribution over a structure — information quite often sought. There are basically two broadly different kinds of measurement situations of primary concern:

- Wire or similarly thin structures on which the current flow is predominately in one direction.
- Surface structures over which the two-dimensional current and charge density are of concern.

One approach for the first measurement situation would be to employ models constructed of hollow tubes through which the sensing cable could be threaded. The sensor itself might consist of a threaded section of tube with an internal cable connector whose outer wall has a circumferential slot and, with the cable's center conductor, terminated against the closed surface of the tube across the slot. This arrangement, similiar to the feed region often postulated for the mathematical treatment of an infinite cylindrical antenna, should permit an accurate current measurement. The loading effect of the sensor, however, might be large enough to require correction.

Surface-current and charge measurements might also be made by employing hollow models and using a small loop or short monopole as their respective sensors introduced through small holes in the surface. Some difficulty could occur because the sensor might respond to unwanted field components or otherwise interact with the measurement environment. However, the former could be controlled by careful construction and the latter by minimizing sensor size consistent with required sensitivity. Various kinds of slot current sensors are available. If it is not possible to drill holes in the model, the sensing cable would have to be attached to the models surface, which might produce unwanted perturbations. Sensor calibration could be achieved by making measurements on the ground plane. Experience based on frequency-domain experimentation could be used wherever possible, but the differences that arise when making broadband transient measurements may render some of these CW techniques inapplicable.

PULSE GENERATORS

The pulse generator is one of the most important links of transient-range instrumentation. It must provide the bandwidth desired at the required signed level and with a minimum of time and amplitude jitter and drift. Alternatives to existing generators are being explored in an attempt to improve generator performance in these areas.

INSTRUMENTATION

Along with the development of improved pulse generators and sensing probes, advances in sampling-oscilloscope technology must be made. While existing sampling scopes have bandwidths extending beyond 10 GHz, higher than our present requirements, some sampling-system components (e.g.,

lumped delay lines) have effective bandwidths below the capabilities of the sampling system itself. These components, therefore, effectively limit the capability of the overall measurement system.

An additional problem area is that of the connectors used to interconnect the sensing probes to the measurement system. Our present transient range employs General Radio type connectors, useable to roughly 7.5 GHz. Although a better class of connectors is available, adapters to all kinds of equipment are not presently available. This situation must be remedied.

COMPUTER SOFTWARE

The acquisition and processing of time-domain data is, of course, very computer oriented. Improvements in the raw data are realized by online filtering, which although presently crude, can have a significant impact on data quality. Further work in this area will be aimed at enhancing the data-acquisition aspect of the range to obtain the highest-quality measurements possible with available instrumentation. This effort may include improving the online filter algorithm, or providing computer compensation for sensor characteristics to obtain more-accurate data.

Offline processing is also an essential part of range operation. We currently use the FFT to derive frequency-domain transfer functions and to scale measured results for different structure sizes, loading values, and EMP-waveform illuminations. One very promising area here is that of using the complex-pole approach for reducing transient measurements to a simpler representation and for performing the transform to the frequency domain. This approach should also allow more effective use of the full free time made available by the range and the processing of very high Q responses. In addition, the kind of data this procedure provides should be well suited for making a measurement data base that is more flexible and convenient to use.

Acknowledgements

Construction of the LLL transient-measurement facility was funded by the Electronics Engineering Department's Engineering Research Division. Developmental work was sponsored by the Defense Nuclear Agency under the guidance of Major William Adams. Technical assistance was provided by Robert Anderson, Jeremy Landt, and Ray Egbert of LLL.

References

1. E. K. Miller, A. J. Poggio, and G. J. Burke, J. Comput. Phys. 12, 24 (1973).

2. J. A. Landt, E. K. Miller, and N. VanBlaricum, "WT-MBA/LLLIB: A Computer Program for the Time-Domain Electromagnetic Response of Thin-Wire Structures," Lawrence Livermore Laboratory, Report UCRL-51585 (1974).

3. J. A. Landt and E. K. Miller, "EMP-Induced Skin Currents on Aircraft," in Proc. Intern. IEEE/AP-S Symp., Atlanta, 1974 (IEEE, Atlanta, GA, 1974) pp. 344-346.

4. C. L. Bennett, H. M. Cronson, and A. M. Nicolson, "Recent Advances in Time-Domain Measurement Techniques," in Proc. USNC/URSI Spring Meeting, Atlanta, 1974 (USNC/URSI, Atlanta, GA, 1974) abstract.

5. A. M. Nicholson, C. L. Bennett, D. Lamensdorf, and L. Susman, IEEE Trans. Microwave Theory and Techniques MTT-20, 3-9 (1972).

6. S. Ramo, J. R. Whinnery, and T. Van Duzer, Fields and Waves in Communication Electronics (John Wiley and Sons Inc., New York, 1965), pp. 462-465.

7. C. R. Trimble, Hewlett-Packard Journal 23, 2 (1968).

8. F. M. Tesche, IEEE Trans. on Ant. & Prop. AP-21 (1), 24 (1973).

WOS/gw